Hydrodynamic description of the long-time tails of the linear and rotational velocity autocorrelation functions of a particle in a confined geometry

Derek Frydel
Max-Planck-Institut für Metallforschung, Heisenbergstrasse 3, D-70569 Stuttgart, Germany

Stuart A. Rice
Department of Chemistry and The James Franck Institute, The University of Chicago, Chicago, Illinois 60637, USA
(Received 25 September 2007; published 28 December 2007)

We report a hydrodynamic analysis of the long-time behavior of the linear and angular velocity autocorrelation functions of an isolated colloid particle constrained to have quasi-two-dimensional motion, and compare the predicted behavior with the results of lattice-Boltzmann simulations. Our analysis uses the singularity method to characterize unsteady linear motion of an incompressible fluid. For bounded fluids we construct an image system with a discrete set of fundamental solutions of the Stokes equation from which we extract the long-time decay of the velocity. For the case that there are free slip boundary conditions at walls separated by H particle diameters, the time evolution of the parallel linear velocity and the perpendicular rotational velocity following impulsive excitation both correspond to the time evolution of a two-dimensional (2D) fluid with effective density $\rho_{2D}=\rho H$. For the case that there are no slip boundary conditions at the walls, the same types of motion correspond to 2D fluid motions with a coefficient of friction $\xi=\pi^2\nu/H^2$ modulo a prefactor of order 1, with ν the kinematic viscosity. The linear particle motion perpendicular to the walls also experiences an effective frictional force, but the time dependence is proportional to t^{-2}, which cannot be related to either pure 3D or pure 2D fluid motion. Our incompressible fluid model predicts correct self-diffusion constants but it does not capture all of the effects of the fluid confinement on the particle motion. In particular, the linear motion of a particle perpendicular to the walls is influenced by coupling between the density flux and the velocity field, which leads to damped velocity oscillations whose frequency is proportional to c_s/H, with c_s the velocity of sound. For particle motion parallel to no slip walls there is a slowing down of a density flux that spreads diffusively, which generates a long-time decay proportional to t^{-1}.

DOI: 10.1103/PhysRevE.76.061404 PACS number(s): 82.70.Dd

I. INTRODUCTION

The molecular chaos assumption, used by Boltzmann as a justification for treating successive binary collisions in a dilute gas as independent dynamical events, leads to the prediction that the velocity autocorrelation function of a molecule decays exponentially. For many years that functional form for the decay was widely assumed to be the same for a molecule in a dense liquid. In 1970 Alder and Wainwright [1] demonstrated, from molecular dynamics simulations, that in a hard sphere fluid at long time the velocity autocorrelation function decays algebraically, i.e., with a power law dependence on time. They interpreted the long-time algebraic decay using a hydrodynamic analysis. That analysis showed that the momentum of a molecule decays by two mechanisms. These mechanisms are emission of a sound wave that rapidly carries away a fraction of the initial momentum and does not contribute at long time, and creation of a velocity field $\mathbf{u}$ that at long time satisfies the diffusion equation $\partial_t\mathbf{u} \approx \nu\nabla^2\mathbf{u}$, thereby generating a dimension dependent long-time decay of the form $(\nu t)^{-d/2}$ in d dimensions, where $\nu = \eta/\rho$ is the kinematic viscosity, η is the shear viscosity, and ρ the liquid density. The diffusive mode is also associated with the creation of vortices that interact back with the moving molecule in a fashion that decreases the rate of decay of the molecular velocity.

A similar prediction pertains to the case of an isolated colloid particle suspended in an unbounded fluid, with dynamics described by the Stokes equation. In an unbounded colloid suspension, the time scales on which the sound propagation mode and the diffusive mode influence the decay of the velocity autocorrelation function are very widely separated, and the former only influences the short time decay of the velocity autocorrelation function of a colloid particle [2]. However, in a bounded colloid suspension, in the limit that the separation of the confining walls is a small multiple of the colloid diameter, the time scales for these modes of decay are not grossly different and the temporal decay of the velocity autocorrelation function is rather complex. Frenkel and co-workers [3,4] have examined the dynamics of a colloid particle suspended in a fluid confined by rigid walls. They showed that, on a hydrodynamic time scale, the velocity autocorrelation function of a colloid particle has a long-time tail whose physical origin and sign are different from that found in an unbounded fluid. Specifically, they showed, from lattice-Boltzmann computer simulations, that at long time the velocity autocorrelation function of the colloid particle decays with a *negative* algebraic tail. They accounted for this temporal behavior using a simple mode-coupling theory that exploits the fact that the sound wave generated by a moving particle becomes diffusive.

This paper is concerned with the hydrodynamic description of the long-time tails of the linear and rotational velocity autocorrelation functions of a colloid particle suspended in a liquid and confined by two planar walls. It builds on the results of a lattice-Boltzmann simulation study of the transition from quasi-two-dimensional to three-dimensional one particle hydrodynamics that we have previously reported [5].

Our analysis complements that of Frenkel and co-workers in several respects. In particular, we analyze the velocity oscillations found in our simulations for the case of linear motion of a colloid perpendicular to the walls, we provide explicit formulas for the long-time tails of the rotational velocity autocorrelation functions for different boundary conditions at the confining walls, and we examine the wall separation dependence of the several autocorrelation function long-time decays.

In the work reported in this paper we use the singularity method to obtain precise expressions describing the long-time decays of the linear and rotational velocity autocorrelation functions of an isolated particle confined between parallel plates. To account for the wall contributions we construct an image system consisting of a discrete set of fundamental solutions to the Stokes equation. We compare these results with those obtained from lattice-Boltzmann simulations for a spherical particle midway between two parallel plates (results reported in Ref. [5]), for different boundary conditions and types of motion. We find that for some types of motion confinement of the fluid can give rise to sound mode contributions to the long-time decay of the velocity autocorrelation function that are not captured by the singularity analysis. The density perturbation caused by an initial particle velocity gives rise to a sound mode whose evolution is governed by a damped wave equation. The characteristic time scale of this process is determined by the speed of sound and in an unbounded fluid this mode does not contribute to the long-time tail of the velocity autocorrelation function. In a confined fluid, for particle motion perpendicular to the walls, density oscillations are generated by the sound modes, with frequency proportional to the speed of sound and inversely proportional to the separation of the walls, the decay of which is determined by the kinematic viscosity. In the case of particle motion parallel to walls at which the no slip boundary condition holds, the sound mode contributions become diffusive and give rise to a negative long-time tail of the velocity autocorrelation function with form $-t^{-2}$ [4].

II. LONG-TIME VELOCITY AUTOCORRELATION FUNCTION

We obtain the linear and angular velocity autocorrelation functions indirectly from the time relaxation of a particle velocity after application of an initial impulsive force. The two quantities are related through the fluctuation-dissipation relation (FD) [5]. For the linear velocity the FD relation is

$$\frac{V_i(t)}{V_i(0)} = \frac{\langle V_i(t)V_i(0)\rangle}{\langle V_i^2\rangle}, \tag{1}$$

where V_i is the Cartesian component of a particle's linear velocity. The same relation obtains for the angular velocity $\Omega_i(t)$. The angular brackets $\langle\cdots\rangle$ denote an equilibrium ensemble average where $\langle V_i^2\rangle = k_BT/M$ and $\langle\Omega_i^2\rangle = k_BT/I$ with M and I the mass and moment of inertia of a particle, respectively.

The long-time behavior of the velocity autocorrelation function is governed by the diffusion of fluid motion to large distances where the force exerted by the particle appears at leading order as a singularity. The singularity representing linear motion is a point force, and that representing angular motion a couplet, that is, the lowest order multipole generated by differentiating a point force. Hydrodynamic singularities set off impulsively are characterized by a power law time decay of the form $t^{-n/2}$, where n increases with increasing multipole order. For the case of an impulsive point force in three-dimensional (3D) fluid the decay is of the form $\propto t^{-3/2}$ and for an impulsive couplet the decay is of the form $\propto t^{-5/2}$. To account for the influence of the wall on the hydrodynamics of a particle in a bounded fluid we construct an image system consisting of a discrete set of fundamental solutions of the Stokes equations. This treatment of the bounding walls disregards the boundary conditions at a particle surface.

III. LONG-TIME BEHAVIOR ASSOCIATED WITH A POINT FORCE IN AN UNBOUNDED FLUID

We define a time dependent point force $\mathbf{b}f(t)\delta(\mathbf{x}-\mathbf{x}_0)$, where $\mathbf{x}_0$ is the location of a point force and $\mathbf{b}f(t)$ is the time dependent vector strength such that $f(t<0)=0$. For $t\geq 0$ and $\mathbf{u}$ sufficiently small this point force generates fluid flow (unsteady Stokes flow) that is determined by the continuity equation for an incompressible fluid and the Stokes equation:

$$\nabla\cdot\mathbf{u} = 0,$$

$$\rho\partial_t\mathbf{u} = \eta\nabla^2\mathbf{u} - \nabla p + \mathbf{b}f(t)\delta(\mathbf{x}-\mathbf{x}_0), \tag{2}$$

where p is the pressure.

To solve for $\mathbf{u}(\mathbf{x},t)$ in Eq. (2) for $t\geq 0$ we Fourier transform in space the Stokes flow and we get

$$\mathbf{k}\cdot\mathbf{u}_\mathrm{k} = 0, \quad \partial_t\mathbf{u}_\mathrm{k} + \nu k^2\mathbf{u}_\mathrm{k} = i\mathbf{k}p_\mathrm{k} + \mathbf{b}f(t).$$

By multiplying the Stokes equation by $\mathbf{k}$ and using the continuity equation we get the expression for pressure,

$$p_\mathrm{k} = \frac{i\mathbf{b}\cdot\mathbf{k}}{k^2}f(t).$$

Noting that $e^{-\nu k^2 t}\partial_t[e^{\nu k^2 t}\mathbf{u}_\mathrm{k}] = \partial_t\mathbf{u}_\mathrm{k} + \nu k^2\mathbf{u}_\mathrm{k}$, the resulting Stokes flow is

$$u_i(\mathbf{x},t) = \frac{b_j}{(2\pi)^d\rho}\int d\mathbf{k}\left(\delta_{ij} - \frac{k_ik_j}{k^2}\right)e^{i\mathbf{k}\cdot(\mathbf{x}-\mathbf{x}_0)} \times \int_0^t dsf(s)e^{-\nu k^2(t-s)}, \tag{3}$$

where we have used the Einstein convention to sum over Cartesian coordinates, and where d denotes dimensionality. The advantage of formulating a velocity flow using an undefined time function $f(t)$ is that it allows a universal definition of a singularity independent of how the singularity strength varies with time. In Fourier space the point force tensor has components $\hat{\mathbf{S}}_{ij} = \delta_{ij} - k_ik_j/k^2$. The higher order singularities are obtained by differentiating $e^{i\mathbf{k}\cdot(\mathbf{x}-\mathbf{x}_0)}$ inside the Fourier integral with respect to $\mathbf{x}$. If $f(t)$ is the Heaviside function,

$$\lim_{t\to\infty}\int_0^t dsf(s)e^{\nu k^2(s-t)} = 1/\nu k^2$$

and Eq. (3) reduces to the steady state point force flow. Alternatively, if $f(t)=e^{-i\omega t}$,

$$\lim_{t\to\infty}\int_0^t dsf(s)e^{\nu k^2(s-t)} = e^{-i\omega t}/(\nu k^2 - i\omega)$$

and Eq. (3) reduces to the oscillatory point force flow. For the impulsive force, $f(t)=\delta(t)$, the solution for the velocity is

$$u_i(\mathbf{x},t) = \frac{b_j}{\rho}\left[\frac{1}{4\pi\nu t}\right]^{d/2} \times\left\{\left(e^{-R^2} - \frac{1}{2}\frac{\gamma[d/2,R^2]}{R^d}\right)\delta_{ij} + \frac{\gamma[d/2+1,R^2]}{R^d}\frac{X_iX_j}{|\mathbf{X}|^2}\right\}. \tag{4}$$

Alternatively, the flow can be represented in terms of the tensor, $u_i=b_jS_{ij}$, where S_{ij} is extracted from Eq. (4). Later in the paper we refer to the definition of S_{ij}. In Eq. (4) $X_i=(x_i-x_{0,i})$, $R=|\mathbf{X}|/\sqrt{4\nu t}$, and $\gamma[n,x]=\int_0^x dtt^{n-1}e^{-t}$ is the lower incomplete gamma function. In the limit $\mathbf{x}\to\mathbf{x}_0$ the tensor term inside the curly brackets reduces to the constant $\frac{d-1}{d}$ and the flow is

$$u_i(\mathbf{x}_0,t) = \frac{d-1}{d}\frac{b_i}{\rho}\left[\frac{1}{4\pi\nu t}\right]^{d/2}. \tag{5}$$

At long time $V_i(t\to\infty)=u_i(\mathbf{x}_0,t)$, i.e., the decay of the particle's linear velocity is the same as the decay of the velocity field induced by a point force whose strength determines the particle velocity at $t=0$. The FD relation, Eq. (1), relates this flow to the linear velocity autocorrelation function (LVACF),

$$\phi^T(t\to\infty) = \langle V_i(t\to\infty)V_i(0)\rangle \approx \langle V_i^2\rangle\frac{d-1}{d}\frac{M}{\rho}\left[\frac{1}{4\pi\nu t}\right]^{d/2}. \tag{6}$$

A similar result was derived in Ref. [8]. A more precise description would give $\nu\to\nu+D$, where D is the diffusion coefficient [9,10]. However, it is usual that $D\ll\nu$ and then Eq. (6) correctly describes the physics of particle velocity decay.

IV. LONG-TIME BEHAVIOR ASSOCIATED WITH A COUPLET IN AN UNBOUNDED FLUID

When rotational motion of a particle is excited by an impulsive torque, the induced fluid flow at long time reduces to that created by an impulsive couplet. We obtain the impulsive couplet directly from the impulsive point force derived in Eq. (4). A couplet is a special case of a point force doublet singularity obtained by differentiating a point force tensor, $\mathbf{B}_{ijk}=\partial_k\mathbf{S}_{ij}$ [6,7]. The resulting flow generated by a point force doublet is $u_i=\mathbf{B}_{ijk}d_{jk}$, where $\mathbf{d}$ is the strength matrix. A point force doublet reduces to a couplet $\mathbf{C}_{ij}$ when the strength matrix $\mathbf{d}$ is antisymmetric. Using Eq. (4) we obtain for the flow generated by an impulsive point force doublet

$$u_i(\mathbf{x},t) = \pi\frac{d_{jk}}{\rho}\left[\frac{1}{4\pi\nu t}\right]^{(d+2)/2}\left\{\left(-2e^{-R^2} + \frac{\gamma[d/2+1,R^2]}{R^{d+2}}\right)\times X_k\delta_{ij} + \frac{\gamma[d/2+1,R^2]}{R^{d+2}}(X_i\delta_{jk}+X_j\delta_{ik}) - 2\frac{\gamma[d/2+2,R^2]}{R^{d+2}}\frac{X_iX_jX_k}{|\mathbf{X}|^2}\right\}. \tag{7}$$

If the matrix $\mathbf{d}$ is antisymmetric (in particular $d_{ik}=-\frac{1}{2}\epsilon_{ijk}L_j$), the expression for the flow reduces to

$$u_i(\mathbf{x},t) = \frac{\pi}{\rho}\left[\frac{1}{4\pi\nu t}\right]^{(d+2)/2}e^{-R^2}\epsilon_{ijk}L_jX_k,$$

from which we extract the angular velocity at $\mathbf{x}=\mathbf{x}_0$,

$$\omega_i(\mathbf{x}_0,t) = L_i\frac{\pi}{\rho}\left[\frac{1}{4\pi\nu t}\right]^{(d+2)/2}. \tag{8}$$

At long time $\Omega_i(t\to\infty)=\omega_i(\mathbf{x}_0,t)$, where $\mathbf{\Omega}(t)$ is the angular velocity of a particle. In Eq. (8) the strength vector is $\mathbf{L}=I\mathbf{\Omega}(0)$. The corresponding angular velocity autocorrelation function (AVACF) is

$$\phi^R(t\to\infty) = \langle\Omega_i^2\rangle\pi\frac{I}{\rho}\left[\frac{1}{4\pi\nu t}\right]^{(d+2)/2}. \tag{9}$$

V. LONG-TIME BEHAVIOR ASSOCIATED WITH A POINT FORCE IN A BOUNDED FLUID

Bounded flow associated with a given singularity can be represented as a superposition of the flow generated by that singularity plus a discrete set of flows that correspond to fundamental solutions of the Stokes equation chosen so as to generate the desired boundary conditions at the wall. For a single planar wall this representation can be achieved by introducing nonphysical singularities (image singularities) outside the physical region [5–7]. This method is the same as that frequently used to determine the influence of boundaries on the field in electrostatics problems. In the application to hydrodynamic flow problems, determination of image singularities is not straightforward for the case of no slip boundary conditions. Blake [11] showed that for steady Stokes flow due to a point force confined by a planar no slip wall, the image consists of three fundamental solutions: a point force, a potential dipole, and a point force doublet. On the other hand, determination of the image singularity is straightforward for free slip boundary conditions. In this case the image singularity forms mirror symmetry with the physical singularity across the planar wall, so the image is the same as the physical singularity with proper orientation.

For a fluid bounded by two parallel walls, representing a solution as a discrete set of fundamental solutions of the Stokes equation has more limited applicability. For example, for the flow generated by a point force between two no slip walls this representation is not feasible and the solution requires integral representation [12]. This limitation does not apply to flow under free slip boundary conditions. Here the image series contains an infinite number of discrete funda-

mental solutions anchored to an infinite number of sites. However, all the singularities in the series are the same as the physical singularity, so the series is well defined. Such is generally the case for any fundamental solution whose image is the same as the physical singularity for fluid bounded by a single wall. For no slip boundary conditions that solution is a couplet since the image is also a couplet rotating in the opposite direction [13].

It needs to be determined if the same procedure carries over to unsteady Stokes flow. For free slip boundary conditions unsteady flow does not change anything as the mirror symmetry argument is still valid. For no slip boundary conditions the situation is more complex. In Ref. [14] it was shown that for oscillating flow the image system for a point force near a no slip wall cannot be constructed as a discrete set of fundamental solutions, although it is possible for steady Stokes flow. In this work we construct a discrete image series for unsteady Stokes flow for singularities between two walls that admit of such construction. In this section we construct the image system for an impulsive point force midway between two parallel free slip walls. Two modes of motion are investigated: parallel and perpendicular to the walls. For convenience we choose the x_3 axis to run perpendicular to the walls. The wall separation is H. For the parallel motion the vector strength is $\mathbf{b}=b\hat{\mathbf{x}}_1$ and the parallel flow is $u_{\|}=u_1$. Expressing the velocity in terms of a tensor, $u_i=(8\pi)^{-1}S_{ij}b_j$, the parallel flow at the singularity for the case of a single wall a distance h away is

$$u_{\|}^{f}=\frac{b_1}{8\pi}[S_{11}(0,0,0)+S_{11}(0,0,2h)],$$

and for the flow between two plates with separation H

$$u_{\|}^{ff}=\frac{b_1}{8\pi}\sum_{n=-\infty}^{\infty}S_{11}(0,0,nH),$$

where S_{ij} is extracted from Eq. (4) and the superscript f denotes the free slip boundary condition. For the single wall case no qualitative change is expected in the functional form of the long-time decay and it can be shown that the prefactor of the functional form only increases by 2, as has been demonstrated in Ref. [15]. On the other hand, the infinite summation term for the two walls case is expected to produce a different functional dependence of the long-time decay. Substituting for S_{ij}, the flow at $\mathbf{x}=\mathbf{x}_0$ is

$$u_{\|}^{ff}(\mathbf{x}_0,t)=\frac{2}{3}\frac{b}{\rho}\left[\frac{1}{4\pi\nu t}\right]^{3/2}\sum_{n=-\infty}^{\infty}g_{\|}^{ff}\left(\frac{n}{\sqrt{\tau}}\right), \tag{10}$$

where

$$g_{\|}^{ff}=\frac{3}{2}e^{-x^2}-\frac{3}{4}\frac{\gamma[3/2,x^2]}{|x|^3}$$

and $\tau=4\nu t/H^2$ is the reduced time. Two contributions are distinguished in Eq. (10); the first represents the time decay of unbounded 3D flow, u_{3D}, and the summation accounts for wall contributions, $\Sigma g_{\|}^{ff}=G_{\|}^{ff}$. In the limit $\tau\to 0$, $G_{\|}^{ff}\to 1$, since at the initial time or at large plate separation 3D flow is recovered. To extract the long-time behavior we use

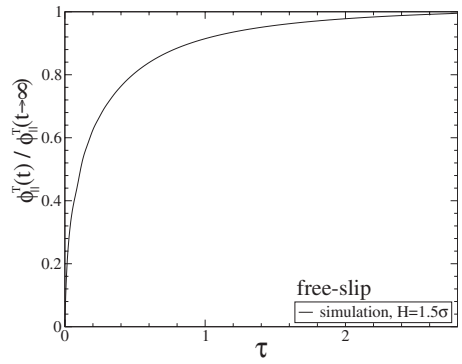

FIG. 1. $\phi_{\|}^{T,ff}$ for a spherical particle midway between two parallel free slip plates obtained from the lattice-Boltzmann simulation [5] normalized by the long-time decay in Eq. (12). $\tau=4\nu t/H^2$ is the reduced time.

the transformation $\Sigma_{n=-\infty}^{\infty}f(n)=\int_{-\infty}^{\infty}dxf(x)\Sigma_{n=-\infty}^{\infty}\delta(x-n)$ and $\Sigma_{n=-\infty}^{\infty}\delta(x-n)=\Sigma_{m=-\infty}^{\infty}e^{i2\pi mx}$. The function $G_{\|}^{ff}$ can now be expressed in the form

$$G_{\|}^{ff}(\tau)=\sum_{m=-\infty}^{\infty}\int_{-\infty}^{\infty}dxg_{\|}^{ff}\left(\frac{x}{\sqrt{\tau}}\right)e^{i2\pi mx}. \tag{11}$$

The mode $m=0$ determines the long-time decay. In fact, it is the only mode that gives algebraic decay; the remaining modes produce exponential decay. The resulting long-time decay of the LVACF is

$$\phi_{\|}^{T,ff}(t\to\infty)=\langle V_{\|}^2\rangle\frac{1}{2}\frac{M}{\rho H}\left[\frac{1}{4\pi\nu t}\right]. \tag{12}$$

Equation (12) represents the algebraic decay of a 2D unbounded fluid with the effective 2D density $\rho_{2D}=\rho H$. The function $G_{\|}^{ff}$ drives a crossover from 3D to 2D fluid behavior. Note that the t^{-1} algebraic decay of the velocity autocorrelation function implies that the diffusion coefficient is undefined (divergent).

We now use the results of the lattice Boltzmann simulations of the behavior of a single spherical particle between two parallel walls, reported in Ref. [5], to test the analytical expressions derived above. In Fig. 1 we plot $\phi_{\|}^{T,ff}$ for a spherical particle confined between two walls with slip boundary conditions, as obtained from the lattice Boltzmann simulations and normalized by the long-time decay described by Eq. (12). At long time the two functions are seen to converge. In Fig. 2 we plot the function $G_{\|}^{ff}$ and its long-time 2D-like limiting behavior as a function of reduced time τ. It is interesting that in the intermediate time, between the 3D- and 2D-like behavior, $G_{\|}^{ff}<1$, indicating that the 3D$\to$2D crossover is not a straightforward process and initially the walls contribute the effective friction to the fluid motion. The 2D-like fluid behavior becomes fully developed for $\tau>0.5$. In addition in Fig. 2 we compare the analytical and simulation results for the ratio $\phi_{\|}^{T,f}/\phi_{3D}^{T}(t\to\infty)$ for a sphere confined between two free slip walls with separation $H=1.5\sigma$. This wall separation is not much larger than the particle diameter σ, and the excluded volume condition at the wall that

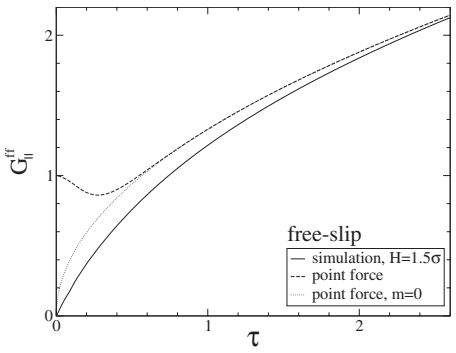

FIG. 2. $G_{\parallel}^{ff}$ (defined by $u_{\parallel}=u_{3D}G_{\parallel}$) for linear motion between two free slip plates as a function of the reduced time $\tau=4\nu t/H^2$.

is accounted for in the simulations but not in the analytical model leads to disagreement with the predictions of the point force singularity model.

To gain better insight of the confinement contributions on a particle motion, it is helpful to consider the case of a point force inside a quasi-one-dimensional square channel moving parallel to the walls with free slip boundary conditions. For the point force placed equidistant from each wall, the function $G_{\parallel}$ is

$$G_{\parallel}(\tau)=\sum_{\mathbf{m}}\int_{-\infty}^{\infty}d^2r g_{\parallel}^{ff}\left(\frac{r}{\sqrt{\tau}}\right)e^{i2\pi\mathbf{r}\cdot\mathbf{m}}, \tag{13}$$

where $\mathbf{m}=m_1\hat{\mathbf{x}}+m_2\hat{\mathbf{y}}$, with m_i denoting integers, corresponds to the reciprocal lattice vector of a discrete image system distributed in space in a square lattice. The lowest algebraic mode, $\mathbf{m}=0$, vanishes [in agreement with Eq. (5) for $d=1$] and, consequently, the long-time behavior is determined by higher order exponential modes. Physically this means that the channel confinement prevents the formation of a vorticity and the walls give rise to the effective friction force. The resulting long-time decay of the LVACF for parallel motion inside a square channel with free slip boundary conditions is

$$\phi_{\parallel}^{T}(t\to\infty)=\langle V_{\parallel}^2\rangle\frac{M}{\rho}\frac{4\sqrt{\pi}}{H^3}\Gamma\left[\frac{1}{2},\frac{4\pi^2\nu t}{H^2}\right], \tag{14}$$

In Eq. (14), $\Gamma[n,x]=\int_x^{\infty}d\gamma\gamma^{n-1}e^{-\gamma}$ is the upper incomplete gamma function. The asymptotic series representation of this gamma function,

$$\Gamma[n,x]=x^{n-1}e^{-x}\left[1+\frac{(n-1)}{x}+\frac{(n-1)(n-2)}{x^2}+\cdots\right],$$

is semiconvergent [16,17]; although it diverges as an infinite series, when x is large an optimal number of terms can be used to obtain any desired degree of approximation. Then for x large, writing $\Gamma[n,x]\cong x^{n-1}e^{-x}$, Eq. (14) can be further reduced to the form

$$\phi_{\parallel}^{T,ff}(t\to\infty)=\langle V_{\parallel}^2\rangle\frac{M}{\rho}\frac{4}{H^2}\left[\frac{e^{-4\pi^2\nu t/H^2}}{(4\pi\nu t)^{1/2}}\right]. \tag{15}$$

Next we investigate linear motion perpendicular to two walls at which there is free slip. The strength vector is now perpendicular to the walls, $\mathbf{b}=b\hat{\mathbf{x}}_3$. For a single wall at a distance h

$$u_{\perp}^{f}=\frac{b_3}{8\pi}[S_{33}(0,0,0)-S_{33}(0,0,2h)],$$

and for two walls separated by a distance H, when the point force is midway between the walls,

$$u_{\perp}^{ff}=\frac{b_3}{8\pi}\sum_{n=-\infty}^{\infty}(-1)^nS_{33}(0,0,nH).$$

When the particle motion is perpendicular to the walls, even when there is only a single wall the algebraic decay of the velocity autocorrelation function is altered since the leading terms cancel and the asymptotic decay is then determined by the next term $\propto t^{-5/2}$ [15]. For the case of fluid interaction with two walls, the function $G_{\perp}^{ff}(\tau)$ that appears in $u_{\perp}^{ff}=u_{3D}G_{\perp}^{ff}$ takes the form

$$G_{\perp}^{ff}=\sum_{n=-\infty}^{\infty}\left\{g_{\perp}^{f}\left[\frac{2n}{\sqrt{\tau}}\right]-g_{\perp}^{f}\left[\frac{1}{\sqrt{\tau}}\left(2n+1-\frac{2\hat{\delta}}{H}\right)\right]\right\},$$

where

$$g_{\perp}^{f}(x)=\frac{3}{2}e^{-x^2}-\frac{3}{4}\frac{\gamma[3/2,x^2]}{|x|^3}+\frac{3}{2}\frac{\gamma[5/2,x^2]}{|x|^3}.$$

We do not limit our investigation to the case that the singularity is located midway between the two walls, so $\hat{\delta}$ is a displacement from the midplane position. Applying the Fourier decomposition to the alternating periodic delta function, we find that the lowest mode $m=0$ vanishes and the next two lowest modes, $m=-1,1$, generate exponential long-time decay. The corresponding long-time behavior of the LVACF is

$$\phi_{\perp}^{T,ff}(t\to\infty)=\langle V_{\perp}^2\rangle\frac{M}{\rho}\frac{\pi}{2H^3}\Gamma\left[-1,\frac{\pi^2\nu t}{H^2}\right]\times\left(1-\cos\left[\pi-\frac{2\pi\hat{\delta}}{H}\right]\right). \tag{16}$$

The incomplete gamma function can be further reduced in the asymptotic limit to the form

$$\phi_{\perp}^{T,ff}(t\to\infty)=\langle V_{\perp}^2\rangle\frac{M}{\rho}\frac{H}{2\pi^3}\left[\frac{e^{-\pi^2\nu t/H^2}}{\nu^2t^2}\right]\times\left(1-\cos\left[\pi-\frac{2\pi\hat{\delta}}{H}\right]\right).$$

The time decay is slowest when the particle is midway between the walls.

In Fig. 3 we plot $\phi_{\perp}^{T,ff}$ obtained from the lattice-Boltzmann simulations for a spherical particle midway between two free slip walls [5] normalized by the long-time decay in Eq. (16), and in Fig. 4 we plot the function $G_{\perp}^{ff}$. The time relaxation exhibits rather complex multitime scale be-

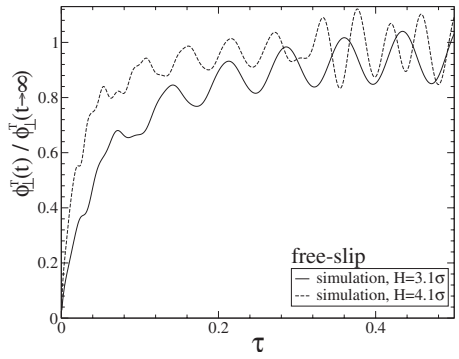

FIG. 3. $\phi_{\perp}^{T,ff}$ as a function of τ for a spherical particle midway between two free slip plates from the lattice-Boltzmann simulation [5] normalized by the long-time decay in Eq. (16). The data for $H=4.1$ is valid within $\tau<0.3$. At $\tau>0.3$ the finite size effects become visible.

havior. In addition to the long-time decay described by Eq. (16) there are damped oscillations not captured by the confined incompressible fluid model. The frequency of oscillations ($\propto tc_s/H$) is related to the wall separation and the speed of sound, c_s (see Fig. 5). This behavior can be traced back to the wave equation of the density perturbation in an unbounded fluid. In a linear fluid the compressibility condition $\partial_t\rho-\rho_0\nabla\cdot\mathbf{u}=0$ leads to a damped wave equation for the evolution of a perturbation of the density,

$$\partial_{tt}\rho = c_s^2\nabla^2\rho + \left(\frac{4}{3}\nu+\zeta\right)\nabla^2\partial_t\rho,$$

where ζ is the bulk viscosity. On the other hand, the coupling between the density flux and the velocity field is of different nature for parallel motion. In Refs. [3,4] the case of motion of a sphere along the long axis of a cylinder and parallel motion of a sphere between two walls with no slip boundary conditions have been investigated. For this motion, the evolution of the density perturbation is governed by the diffusion equation, rather than the wave equation, with diffusion coefficient determined by the effective friction caused by the no slip boundary conditions at the walls. The initial density perturbation introduced by an impulsive force causes a back flow that produces a negative long-time decay with form $\propto -t^{-2}$.

For the case that the particle motion is parallel to and midway between the plates, the velocity component perpendicular to the walls vanishes in the midplane and the linear incompressible hydrodynamic equation reduces to

$$\partial_t\mathbf{u}_{\parallel} = \nu\nabla_{\parallel}^2\mathbf{u}_{\parallel} - \frac{1}{\rho}\nabla_{\parallel}p + \left.\nu\frac{\partial^2\mathbf{u}_{\parallel}}{\partial x_3^2}\right|_{x_3=0},$$

which is the equation of motion of a 2D fluid with additional term $\nu\partial^2\mathbf{u}_{\parallel}/\partial x_3^2$. When the fluid is subject to free slip boundary conditions this term vanishes at long time and the equation of motion of a 2D fluid is retrieved. On the other hand, when the fluid is subject to no slip boundary conditions this term at long time represents a friction force $\nu\partial^2\mathbf{u}_{\parallel}/\partial x_3^2\approx\xi\mathbf{u}_{\parallel}$ [19]. We show in the next section that for the case of rotational motion of the particle the friction coefficient is $\xi=\pi^2\nu/H^2$ (which agrees with that for the parallel motion [18]). Based on this intuitive description, we expect the long-time decay of the velocity parallel to no slip walls to be

$$u_{\parallel}^{nn} = A\frac{b}{\rho H}\frac{e^{-\pi^2\nu/H^2}}{4\pi\nu t},$$

where the constant A is of order 1. For a compressible linear fluid the density then would satisfy the equation

$$\partial_{tt}\rho + \frac{\pi^2\nu}{H^2}\partial_t\rho = c_s^2\nabla_{\parallel}^2\rho + \left(\frac{4}{3}\nu+\zeta\right)\nabla_{\parallel}^2\partial_t\rho.$$

If the friction coefficient is large this equation reduces to the diffusion equation

$$\partial_t\rho = \frac{c_s^2H^2}{\pi^2\nu}\nabla_{\parallel}^2\rho.$$

The exact value for the diffusion coefficient obtained and confirmed by simulation in Refs. [3,4] is $c_s^2H^2/(12\nu)$, which has the same functional dependence on the relevant system parameters but differs by a numerical constant. The intuitive model thus does capture the essential physics of the situation being described.

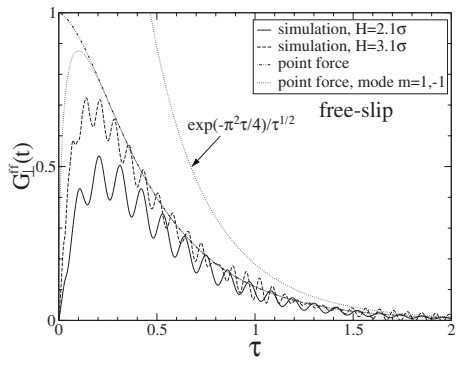

FIG. 4. $G_{\perp}^{ff}$ as a function of a reduced time τ for a point force and a spherical particle at different plate separations.

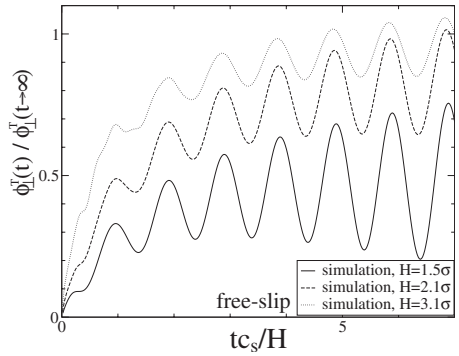

FIG. 5. $\phi_{\perp}^{T,ff}$ as a function of tc_s/H for a spherical particle midway between two free slip plates from the lattice-Boltzmann simulation normalized by the long-time decay in Eq. (16).

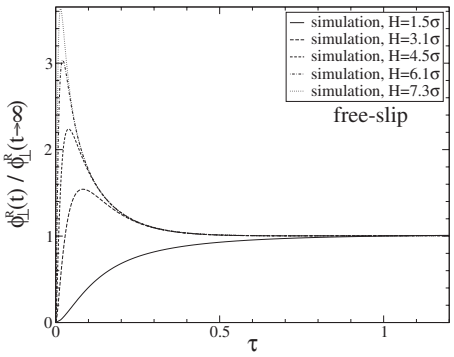

FIG. 6. $\phi_\perp^{R,ff}$ for a spherical particle midway between two free slip plates from the lattice-Boltzmann simulation normalized by a long-time decay in Eq. (17).

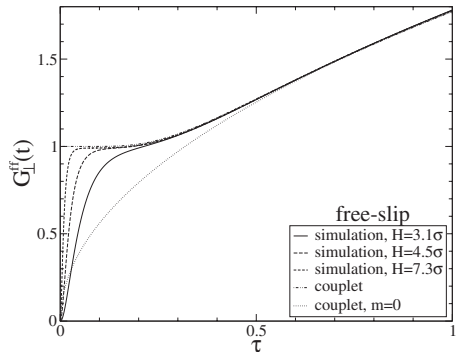

FIG. 7. $G_\perp^{ff}$ for rotational motion between two free slip plates as a function of the reduced time τ.

VI. LONG-TIME BEHAVIOR ASSOCIATED WITH A COUPLET SOURCE IN A BOUNDED FLUID

We now investigate the time decay of the velocity autocorrelation function corresponding to motion induced by a couplet rotating along an axis perpendicular to the walls. The image technique for this motion is applicable to no slip boundary conditions. A single free slip wall does not change the functional dependence of the long-time behavior associated with perpendicular rotation [15] (see Fig. 5). The function $G_\perp^{ff}(\tau)$ [here defined by $\omega_\perp = \omega_{3D}(t) G_\perp(\tau)$] for perpendicular rotation of a couplet that is midway between two walls with free slip boundary conditions is

$$G_\perp^{ff} = \sum_{n=-\infty}^{\infty} \exp\left[-\frac{n^2}{\tau}\right].$$

Then the long-time decay of the corresponding velocity autocorrelation function is

$$\phi_\perp^{R,f}(t\to\infty) = \langle \Omega_\perp^2 \rangle \pi \frac{I}{\rho H}\left[\frac{1}{4\pi\nu t}\right]^2, \tag{17}$$

which describes the long-time decay of a 2D fluid with the effective 2D density $\rho_{2D}=\rho H$. This prediction for the long-time decay is found to agree with the results obtained from the lattice-Boltzmann simulations (Fig. 6). The plot of $G_\perp^{ff}$ for a couplet, displayed in Fig. 7, shows a plateau for $\tau < 0.2$ for which 3D-like behavior is sustained. The function $G_\perp^{ff}$ obtained from the simulation for different wall separations shows convergence to the predicted couplet results as the wall separation increases.

On the other hand, the interaction of the fluid with one wall with a no slip boundary condition does change the functional dependence of the long-time behavior associated with perpendicular rotation; the long-time form of the algebraic decay changes from to $\propto t^{5/2} \to \propto t^{7/2}$ [15]. The function $G_\perp^{nn}$ for a couplet midway between the two walls at which the no slip boundary condition holds is

$$G_\perp^{nn} = \sum_{n=-\infty}^{\infty} (-1)^n \exp\left[-\frac{n^2}{\tau}\right],$$

which gives rise to the following long-time decay of the AVACF:

$$\phi_\perp^{R,n}(t\to\infty) = \langle \Omega_\perp^2 \rangle 2\pi \frac{I}{\rho H}\left[\frac{1}{4\pi\nu t}\right]^2 e^{-\pi^2 t\nu/H^2}. \tag{18}$$

In this case the long-time decay is twice the time decay of a 2D fluid with friction coefficient $\xi=\pi^2\nu/H^2$. Comparisons with the data obtained from the lattice Boltzmann simulations, shown in Figs. 8 and 9, verify the predicted long-time decay. Rotational motion of a particle in a confined geometry is not effected by density fluctuations as the time relaxation of this mode of motion is determined by the relaxation of the vorticity.

VII. SUMMARY

In this paper we have used the singularity method to characterize unsteady linear motion of an incompressible fluid. To analyze the behavior of a particle in a bounded fluids we constructed an image system with a discrete set of fundamental solutions of the Stokes equation from which we extracted the long-time decay of the velocity. The singularities

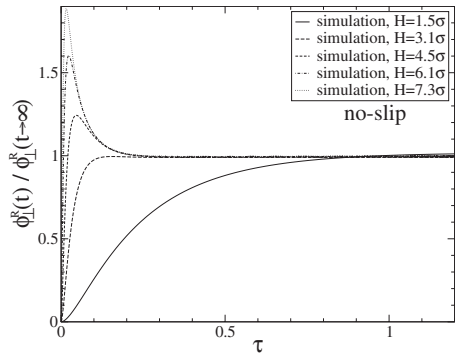

FIG. 8. $\phi_\perp^{R,nn}$ for a spherical particle midway between two no slip plates from the lattice-Boltzmann simulation normalized by a long-time decay in Eq. (17).

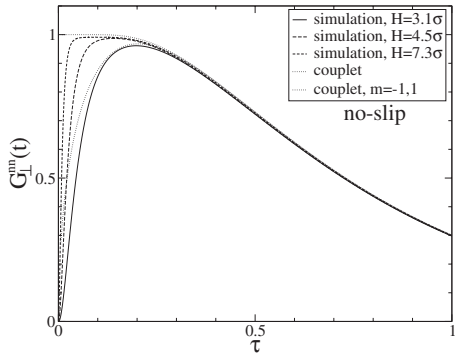

FIG. 9. $G_{\perp}^{nn}$ for rotational motion between two no slip plates as a function of the reduced time τ.

were taken to be impulsive forces or torques and their time evolutions were mapped onto the long-time relaxation of a solid spherical particle set in motion impulsively. Within this model, for the case that there are free slip boundary conditions at the confining walls, the time evolution of the parallel linear velocity and the perpendicular rotational velocity correspond to the long-time algebraic evolution of a 2D fluid with the effective density $\rho_{2D}=\rho H$. In addition we found that for parallel linear motion inside a channel with free slip boundary conditions the long-time decay is exponential with the effective friction force $4\pi^2\nu/H^2$, as in this type of confinement a vorticity which controls the algebraic decay is prevented from developing. For the case that there are no slip boundary conditions at the confining walls, the same types of motion correspond to a 2D fluid motion with a frictional force whose coefficient of friction is $\pi^2\nu/H^2$ and with additional prefactor of order 1. The perpendicular linear motion also experiences an effective friction force coupled to the long-time dependence proportional to t^{-2}, which cannot be related to either 3D or 2D fluid motion. The time evolutions predicted by our hydrodynamic arguments agree with those obtained from lattice-Boltzmann simulations.

Our incompressible fluid model does not capture all of the effects of fluid confinement on embedded particle motion if a vorticity is prevented from developing and so other processes control the long-time behavior. In particular, the confinement affects the coupling between the density flux and the velocity field (first investigated in Refs. [3,4]), and thereby the linear motion of a particle perpendicular to the walls and the linear motion of a particle parallel to walls at which there is a no slip boundary condition. For perpendicular motion the effect of the density coupling appears as additional velocity oscillations whose frequency is proportional to $\propto c_s/H$ and whose time evolution is governed by a damped wave equation. For parallel no slip motion the confinement causes slowing down of a density flux that spreads diffusively. This diffusive density flux determines the long-time decay proportional to $-t^{-2}$, for two wall confinement, and $-t^{-3/2}$, for the channel type of confinement [3,4]. The theory for incompressible fluids, however, predicts correct self-diffusion constants (which can be obtained from the Green-Kubo expression) and is not affected by fluid compressibility [20].

ACKNOWLEDGMENTS

This research was supported by the National Science Foundation funded MRSEC Laboratory at the University of Chicago.

[1] B. J. Alder and T. E. Wainwright, Phys. Rev. A **1**, 18 (1970).
[2] R. Zwanzig and M. Bixon, Phys. Rev. A **2**, 2005 (1970).
[3] M. H. J. Hagen, I. Pagonabarraga, C. P. Lowe, and D. Frenkel, Phys. Rev. Lett. **78**, 3785 (1997).
[4] I. Pagonabarraga, M. H. J. Hagen, C. P. Lowe, and D. Frenkel, Phys. Rev. E **59**, 4458 (1999).
[5] D. Frydel and S. Rice, Mol. Phys. **104**, 1283 (2006).
[6] C. Pozrikidis, *Boundary Integral and Singularity Methods* (Cambridge University Press, New York, 1992).
[7] C. Pozrikidis, *Introduction to Theoretical and Computational Fluid Dynamics* (Oxford University Press, New York, 1997).
[8] R. Hocquart and E. J. Hinch, J. Fluid Mech. **137**, 217 (1983).
[9] J. P. Hansen and I. R. McDonald, *Theory of Simple Liquids*, 2nd edition (Academic Press, New York, 1986).
[10] A. J. Masters and T. Keyes, J. Stat. Phys. **39**, 215 (1985).
[11] J. R. Blake, Prog. Colloid Polym. Sci. **70**, 303 (1971).
[12] N. Liron and S. Mochon, J. Eng. Math. **10**, 287 (1976).
[13] J. R. Blake and A. T. Chwang, J. Eng. Math. **8**, 23 (1974).
[14] C. Pozrikidis, Phys. Fluids A **1**, 1508 (1989).
[15] I. Pagonabarraga, M. H. J. Hagen, C. P. Lowe, and D. Frenkel, Phys. Rev. E **58**, 7288 (1998).
[16] G. B. Arfken and H. J. Weber, *Mathematical Methods for Physicists* (Elsevier Academic Press, New York, 2005).
[17] P. Amore, Europhys. Lett. **71**, 1 (2005).
[18] L. Bocquet and J.-L. Barrat, J. Phys.: Condens. Matter **8**, 9297 (1996).
[19] S. Ramaswamy and G. F. Mazenko, Phys. Rev. A **26**, 1735 (1982).
[20] L. Bocquet and J.-L. Barrat, Europhys. Lett. **31**, 455 (1995).